PKCε inhibition prevents ischemia-induced dendritic spine impairment in cultured primary neurons

CHENJIE GE[1*], XUEFENG WANG[2*], YUNHONG WANG[2], LILEI LEI[1], GUOHUA SONG[1], MINCAI QIAN[1] and SHILIANG WANG[1]

[1]Department of Psychiatry, Huzhou Third Municipal Hospital, The Affiliated Hospital of Huzhou University, Huzhou, Zhejiang 313000; [2]WuXi AppTec Co., Ltd., Shanghai 200131, P.R. China

Received September 29, 2022; Accepted January 31, 2023

DOI: 10.3892/etm.2023.11851

Abstract. Brain ischemia is an independent risk factor for Alzheimer's disease (AD); however, the mechanisms underlining ischemic stroke and AD remain unclear. The present study aimed to investigate the function of the ε isoform of protein kinase C (PKCε) in brain ischemia-induced dendritic spine dysfunction to elucidate how brain ischemia causes AD. In the present study, primary hippocampus and cortical neurons were cultured while an oxygen-glucose deprivation (OGD) model was used to simulate brain ischemia. In the OGD cell model, *in vitro* kinase activity assay was performed to investigate whether the PKCε kinase activity changed after OGD treatment. Confocal microscopy was performed to investigate whether inhibiting PKCε kinase activity protects dendritic spine morphology and function. G-LISA was used to investigate whether small GTPases worked downstream of PKCε. The results showed that PKCε kinase activity was significantly increased following OGD treatment in primary neurons, leading to dendritic spine dysfunction. Pre-treatment with PKCε-inhibiting peptide, which blocks PKCε activity, significantly rescued dendritic spine function following OGD treatment. Furthermore, PKCε could activate Ras homolog gene family member A (RhoA) as a downstream molecule, which mediated OGD-induced dendritic spine morphology changes and caused dendritic spine dysfunction. In conclusion, the present study demonstrated that the PKCε/RhoA signalling pathway is a novel mechanism mediating brain ischemia-induced dendritic spine dysfunction. Developing therapeutic targets for this pathway may protect against and prevent brain ischemia-induced cognitive impairment and AD.

Correspondence to: Dr Shiliang Wang, Department of Psychiatry, Huzhou Third Municipal Hospital, The Affiliated Hospital of Huzhou University, 2088 TiaoXi Road (East), WuXing, Huzhou, Zhejiang 313000, P.R. China
E-mail: wangsl1177@hz3rd-hosp.cn

*Contributed equally

Key words: Alzheimer's disease, protein kinase Cε, oxygen-glucose deprivation, brain ischemia, dendritic spine

Introduction

Brain ischemia episodes facilitate the onset of dementia, with 10% of patients developing dementia and cognitive impairment soon after their first stroke (1). Studies have indicated that ischemia and the primary type of dementia, Alzheimer's disease (AD), are statistically correlated (2-4). For example, a previous clinical study revealed that stroke is an independent risk factor for AD (4). Numerous animal studies have also suggested a higher occurrence rate of AD following brain ischemia/stroke (5,6). Thus, it is important to investigate the molecular association between brain ischemia and AD to reduce AD occurrence following a brain ischemia.

Ischemic neurotoxicity leads to extensive neuronal impairments in certain regions of the forebrain, such as the cortex and hippocampus. These regions are associated with cognitive function (7). A previous study showed that dendritic spine dysfunction is the earliest neurotoxicity symptom following brain ischemia (8). More importantly, dendritic spine dysfunction is a biomarker predicting AD occurrence (9,10). Based on these previous findings, it was hypothesized that protecting dendritic spine function following brain ischemia might relieve neuronal death following stroke, which might ultimately reduce AD occurrence following brain ischemia.

The function and dynamics of dendritic spines are tightly regulated by cytoskeletal proteins, such as microtubules and their upstream regulator, Rho-GTPases (11). Members of the protein kinase C (PKC) family are known for their functions in regulating the activity of Rho-GTPase. The ε isoform of PKC (PKCε) has been found to regulate the cytoskeleton in cardiocytes and to protect cells from mitochondria damage following myocardial ischemia (12). However, the role of PKCε in neuronal cells following ischemia remains unclear. Oxygen-glucose deprivation (OGD) is a well-established cell-based method for simulating brain ischemia *in vitro* (13) that has been used extensively in basic and preclinical stroke studies (14-16). In the present study, OGD was applied to primary hippocampus and cortical neurons to investigate the role of PKCε in dendritic spine dysfunction following ischemia. The results of the present study may suggest novel

therapeutic targets for cognitive function protection following brain ischemia.

Materials and methods

Rat euthanasia. Pregnant Sprague-Dawley rats at E17 were purchased from the vivarium facility of WuXi AppTec Co., Ltd. Upon arrival, rats were left in the procedure room overnight and euthanized on E18. A total of 20 pregnant female rats (age between 8-12 weeks and body weight around 250 g were used. For euthanasia, rats were put in a large transparent plastic box for 10 min and inhalant anaesthesia was performed by placing a 50-ml centrifuge tube containing 15 ml liquid isoflurane (99.9%; cat. no. H19980141; Ruitaibio Co.) into the plastic box. The plastic box was then sealed with the lid to avoid the evaporation of isoflurane. The final isoflurane percentage was 3% for both induction and maintenance of anaesthesia. Generally, rats would be anaesthetized in 10-15 min. Subsequently, the abdomen skin of anaesthetized rats was sterilized with 70% ethanol. Following sterilization, an incision was made along the midline of the abdomen using clinical scissors, from the small intestine up to the heart. Finally, rats were sacrificed by cutting off a piece of the left heart ventricle and decapitation with surgical scissors. Death was verified by loss of heartbeat. Rats were under anaesthesia for the whole euthanasia process. Embryos were collected into a 100-cm dish for hippocampus and cortex dissection in a tissue culture room.

The animal welfare and husbandry were conducted at the vivarium room of WuXi AppTec Co., Ltd. Pregnant rats were housed in separate cages, with *ad libitum* access to food and water supply, and 12/12-h light/dark cycles at 24-26˚C and 30-70% humidity. Animal health was monitored daily. Physiological or behavioural symptoms, such as severe pain, overt distress, moribund and beyond the point where recovery appears reasonable, were used as humane endpoint criteria resulting in animal euthanasia to minimize suffering by inhalation of 100% CO_2 with 70% chamber volume /min influx rate. Fetuses were euthanized by decapitation with surgical scissors.

Primary neuronal culture. The present study was collaborative research between the Huzhou Third Municipal Hospital, The Affiliated Hospital of Huzhou University (Huzhou, Zhejiang, China) and WuXi AppTec Co., Ltd. Procedures involving animals were approved by the Institutional Animal Care and Use Committee of the WuXi AppTec Co., Ltd. company at the Qidong (Jiangsu, China) site (IACUC approval no. GP01-QD089-2022v1.0). Cell culture was performed as previously described (17). In brief, before dissection, 35-mm cell culture dishes were pre-treated with 1 ml Poly-L-Lysine (0.5 mg/ml; cat. no. P4707; MilliporeSigma) overnight at 37˚C and washed with sterile water three times. Pregnant Sprague-Dawley rats at embryonic day 18 (E18) were sacrificed and embryos were decapitated with surgical scissors and dissected for hippocampus and cortex neuron culture. Low-density hippocampus ($1x10^4$ cells for a total of three coverslips/35 mm dish) or high-density cortical cultures ($1x10^7$ cells/35 mm dish) were grown in neurobasal medium (cat no. 21103049; Invitrogen; Thermo Fisher Scientific, Inc.) supplemented with 1X B-27 (cat no. 17504044; Invitrogen; Thermo Fisher Scientific, Inc.) and 2 mM GlutaMAX™ (cat no. 35050061; Invitrogen; Thermo Fisher Scientific, Inc.). At 6 days *in vitro* (DIV), primary neurons were transfected with enhanced green fluorescent protein (eGFP) plasmids (pcDNA3-eGFP, cat no. 13031 Addgene) for visualization using calcium phosphate precipitation, as previously described (17). In brief, 2 μg eGFP plasmid was transfected overnight at 37˚C using Calcium Phosphate Transfection Kit (cat no. K278001, Thermo Fisher). Fresh medium was added and primary neurons were incubated in 37˚C until use on DIV 17.

OGD model establishment. The OGD model was established as previously described (18). To simulate ischemic stroke *in vitro*, primary neurons were washed gently with PBS (pH 7.4; cat. no. 10010023; Invitrogen; Thermo Fisher Scientific, Inc.) twice. Neurons were cultured in DMEM with no glucose (cat. no. 11966025; Invitrogen; Thermo Fisher Scientific, Inc.) or supplements and incubated in a humidified oxygen control CO_2 incubator (type-i160; Thermo Fisher Scientific, inc.) with 1% O_2, 5% CO_2 and 94% N_2 at 37˚C for 2 h.

Confocal imaging and quantification. Confocal images were obtained using a Zeiss LSM 800 confocal microscope [Carl Zeiss IMT (Shanghai) Co., Ltd.] with an x63 oil objective (1.0 numerical aperture) with a sequential acquisition setting. Following OGD treatment, primary hippocampus neurons were washed with PBS and fixed with 4% paraformaldehyde at room temperature for 20 min (cat. no. P0099; Beyotime Institute of Biotechnology). Fixed cells were visualized with 488 nm excitation for enhanced green-fluorescent protein. Up to 10 positive neurons were observed per dish. Dendritic spines resembled mushroom-shaped protrusions. Spine length and width were measured using ImageJ (version 1.50i; National Institutes of Health). Spine length was defined as the distance from the tip of the spine head to the point where the spine starts to grow at the dendrite. Spine width was defined as the maximal width of the spine head perpendicular to the long axis of the spine neck.

For PKCε inhibiting assay, PKCε-specific inhibiting peptide, EAVSLKPT, was used here (cat no. 539522; MilliporeSigma). In brief, hippocampus neurons were transfected with 2 μg of eGFP plasmid at DIV6 and treated with 1 mM inhibitor at DIV16. After 24 h treatment at 37˚C, cells were moved to an OGD chamber for 2 h. After OGD treatment, cells were fixed and observed under confocal microscope in the way as stated above.

While performing quantifications, all green positive neurons in each dish that have intact cell membrane were imaged and used for quantification. All dendritic spines identified on each imaged neuron were quantified for number, length and width. There were at least 30 positive neurons from 3-5 repeated experiments used for quantification and 1,200-1,500 dendritic spines were quantified in total in each group (50-70 spines per neuron). The quantifications were performed by two individuals (LL and GS) who were blind to the experimental conditions and the results were averaged.

Cell viability assay. The viability of primary neurons was detected via MTT assay (cat no. ST1537; Beyotime Institute of Biotechnology), according to the manufacturer's instructions.

Briefly, following the OGD treatments, primary cortical neurons were washed with PBS and incubated with MTT reagent (50 μl/well in a 6-well-plate) at 37˚C for 4 h. 100 μl DMSO was added to dissolve the formazan. Absorbance was measured at 450 nm using a plate reader (BioTek Synergy HT Multi-Mode Microplate reader, BioTek China).

Rho-GTPase activity assay. The rho-GTPase activity was measured using different G-LISA activation assay kits (cat. nos. BK124 for active RhoA, BK128 for active Rac1 and BK127 for CDC42; Cytoskeleton, Inc.) following the manufacturer's instructions. Briefly, high-density cortical neurons with OGD treatment were lysed using the lysis buffer supplied with the kits. A total of 25 μg total protein/group was loaded into each well and then incubated with primary and secondary antibodies that supplied with the G-LISA kits (cat. nos. BK124 for active RhoA, BK128 for active Rac1 and BK127 for CDC42; Cytoskeleton, Inc.). According to manufacturer's instruction, the primary antibody can incubate at room temperature for 1 h and then the secondary antibody can incubate at room temperature for 1 h. The reaction plate was incubated with a detection solution at room temperature for 30 min according to manufacturer's instruction and the level of activation was determined by measuring the absorbance at 490 nm (BioTek Synergy HT Multi-Mode Microplate reader, BioTek China).

Electrophysiology recording. Electrophysiology whole-cell recordings were performed in voltage-clamp mode using a MultiClamp 700B amplifier (Molecular Devices, LCC) at a sampling frequency of 50 kHz and recorded signals were digitized using a Digidata 1440 digitizer (Molecular Devices, LCC). Patch pipettes were pulled from borosilicate glass and had a resistance of 3-5 MΩ when filled with standard intracellular solution (95.0 K-gluconate, 50.0 KCl, 10.0 HEPES, 4.00 Mg-ATP, 0.3 NaGTP and 10.0 mM phosphocreatine; pH 7.2, 300 mOsm). Miniature excitatory postsynaptic current (mEPSC) was measured in rat hippocampal neurons following OGD at room temperature in artificial cerebrospinal fluid (126.0 NaCl, 2.5 KCl, 10.0 glucose, 1.25 NaH_2PO_4, 2.0 $MgCl_2$, 2.0 $CaCl_2$ and 26.0 mM $NaHCO_3$) with 0.5 μM tetrodotoxin (Sigma-Aldrich; Merck KGaA).

In vitro PKCε kinase activity. PKCε kinase activity was measured using PKCε Kinase Enzyme System (cat. no. V4037; Promega Corporation), according to the manufacturer's instructions. Briefly, high-density cortical neurons with OGD treatment were lysed with RIPA buffer (cat. no. P0013B; Beyotime Institute of Biotechnology) and 100 μg total protein/group was then used for incubation with 5 μM ATP and 0.1 μg/μl substrate for 60 min at room temperature. A total of 25 ng purified PKCε was used as the positive control. Following incubation, ADP-Glo™ was added and incubated at room temperature for 40 min according to manufacturer's instructions. Luminescence signals were detected using a microplate reader (BioTek Synergy HT Multi-Mode microplate reader, BioTek China).

Western blotting. Following OGD treatment, primary cortical neurons were washed twice with PBS and cells were lysed using a protein lysis buffer (cat. no. P0013B; Beyotime Institute of Biotechnology) in a cold room at 4˚C for 10 min. Following centrifugation (10,000 x g for 10 min at 4˚C), the supernatant was transferred to a new tube and protein concentration was quantified using a Pierce BCA protein assay (cat. no. 23225; Thermo Fisher Scientific, Inc.). An equal amount of protein from each group was denatured at 95˚C for 5 min and 50 μg protein/lane was separated by SDS-PAGE on a 10% gel. Following the transfer onto a 0.45-μm PVDF membrane (cat no. 88518; Thermo Fisher Scientific, Inc.), PVDF membranes were blocked with 5% BSA (cat. no. ST025; Beyotime Institute of Biotechnology) for 1 h at room temperature. Following blocking, membranes were incubated with a primary antibody overnight in a cold room at 4˚C and with a secondary antibody for 1 h at room temperature. The following primary antibodies were used: Rabbit anti-total-Ras homolog family member A (RhoA; cat. no. 2117; 1:2,000; Cell Signaling Technology, Inc.); rabbit anti-total-Rac Family Small GTPase 1 (Rac1; cat. no. 2465; 1:2,000; Cell Signaling Technology, Inc.); rabbit anti-total-cell division cycle 42 (CDC42; cat. no. 2466; 1:1,000; Cell Signaling Technology, Inc.), rabbit anti-β Tubulin (cat. no. 2416; 1:5,000, Cell Signaling Technology, Inc.), and rabbit anti-PKCε (cat. no. 2683; 1:1,000; Cell Signaling Technology, Inc.). The secondary antibodies were horseradish peroxidase anti-rabbit IgG (cat. no. 7074; 1:5,000; Cell Signaling Technology, Inc.). Protein bands were visualized using Pierce™ ECL Western Blotting Substrate (cat no. 32209; Thermo Fisher Scientific, Inc.) and developed in a dark room using X-OMAT BT film (cat. no. FF057; Beyotime Institute of Biotechnology). The quantification of the bands was performed using ImageJ software (version 1.50i; National Institutes of Health).

Statistical analysis. Results were analyzed using GraphPad Prism Software Version 6.0 (GraphPad Software, Inc.; Dotmatics). All data are presented as the mean ± standard deviation, with replicates from 3 to 10. Statistical comparisons were performed using unpaired Student's t test (for comparisons between two groups), one-way ANOVA followed by Tukey's post hoc test (for comparisons between 3 groups) or two-way ANOVA followed by Tukey's post hoc test (for quantification of spine length and width). All electrophysiological data were analyzed using Clampfit (Molecular Device, LLC). $P<0.05$ was considered to indicate a statistically significant difference.

Results

OGD damages the morphology and function of the dendritic spine in primary hippocampus neuronal culture. To investigate how ischemia interrupts dendritic spine morphology and function, an acute OGD model was induced in cultured primary hippocampus neurons. The OGD treatment is an established *in vitro* method to simulate severe hypoxic and ischemic conditions by withdrawing glucose in culture media while limiting the oxygen supply to 1%. Primary hippocampus neurons were transfected with eGFP plasmid for visualization at DIV6 and transferred into a hypoxia chamber at DIV17 with DMEM without glucose. According to a previous study (19), most of the dendritic spines in cultured hippocampus neurons mature at DIV17. After 2 h treatment, hippocampus neurons

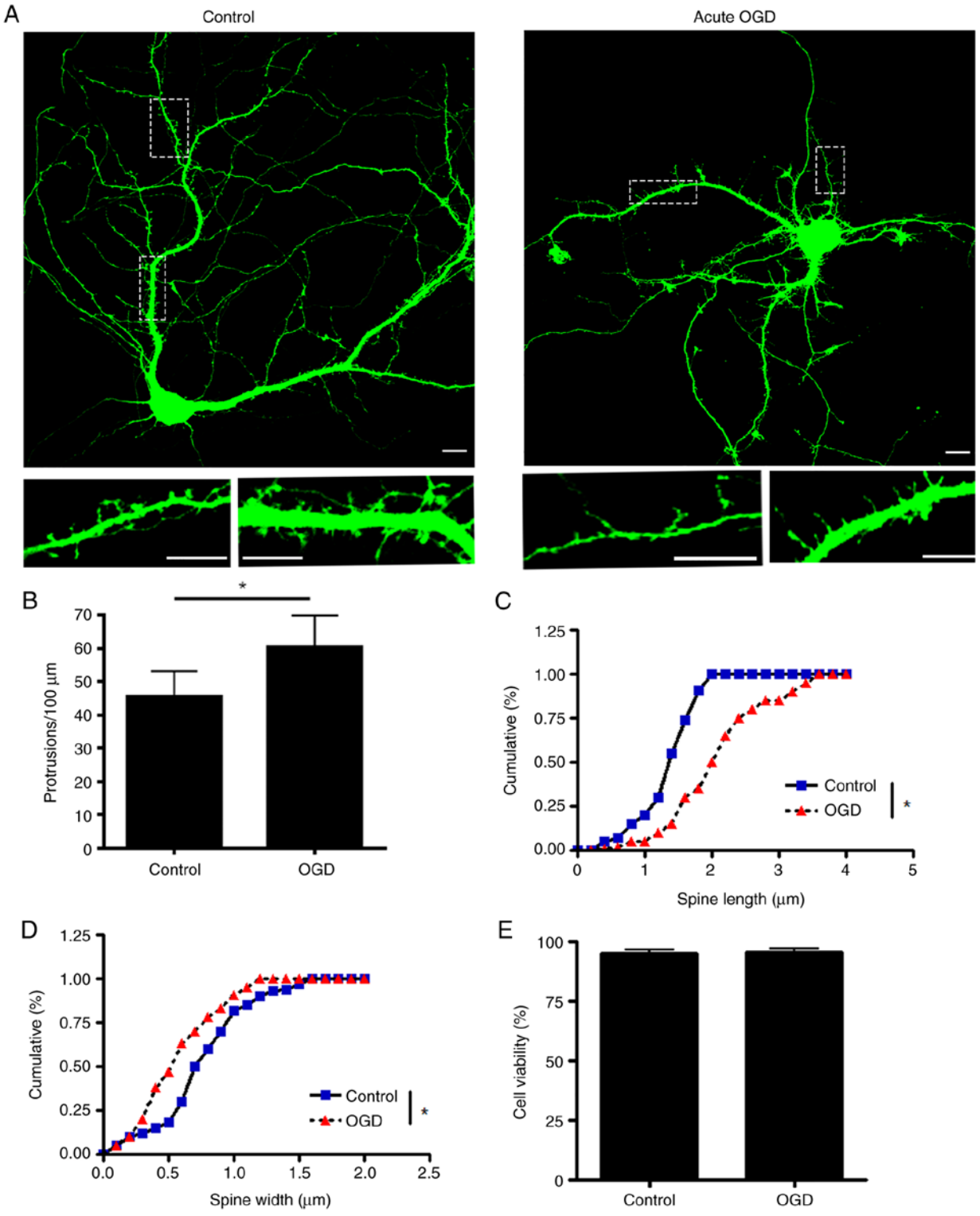

Figure 1. Acute OGD treatment impairs dendritic spine morphology. (A) Primary hippocampus neurons were transfected with enhanced green fluorescent protein. Upper images represent neurons treated with OGD and visualized under confocal microscopy at DIV17 (scale bar, 10 μm). Lower images are magnified image from the doted square regions of the upper image. (B) Number of protrusions. Spine (C) length and (D) width (n=1,200-1,500 spines from ≥20 neurons). (E) High-density cortical neurons were treated with OGD at DIV17 and tested with MTT (n=3 batches of neurons). *P<0.05. OGD, oxygen-glucose deprivation; DIV, days *in vitro*.

were fixed and imaged using a confocal microscope to analyse the morphology of dendritic spines. Following acute phase OGD, total protrusions in the dendrites were significantly increased, while the number of mature dendritic spines was decreased. The mean width of the spine head was decreased (Fig. 1A-D), which indicated that the dendritic spine underwent shrinking. Furthermore, acute OGD treatment did not induce significant neuronal death (Fig. 1E). Finally, electrophysiology was performed to measure the function of the synapses. The frequency of mEPSC was significantly decreased following

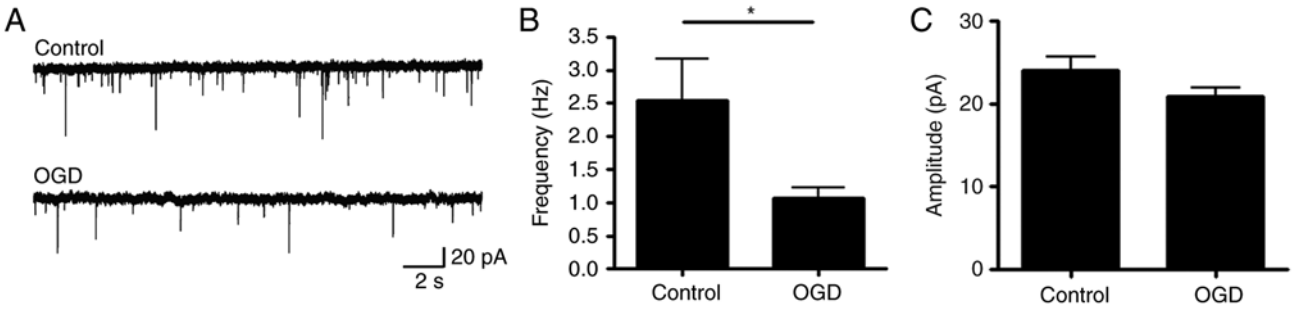

Figure 2. Acute OGD treatment impairs synapse function. (A) Miniature excitatory postsynaptic current was recorded on cultured primary hippocampus neurons with or without OGD treatment. (B) Current frequency. (C) Amplitude (n=20-30 neurons). *P<0.05. OGD, oxygen-glucose deprivation.

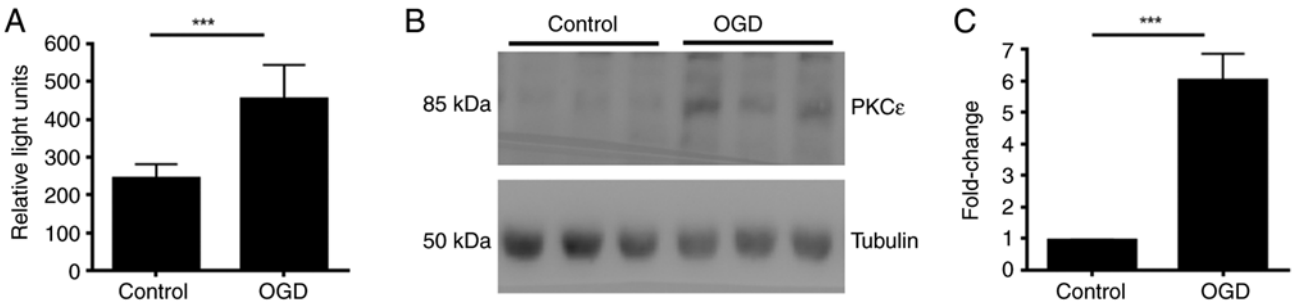

Figure 3. Acute OGD upregulates PKCε protein expression and kinase activity. (A) High-density cortical neurons were treated with OGD at DIV17. Neurons were lysed to detect kinase activity. (B) Neurons were then lysed to detect (C) protein expression. ***P<0.001. PKCε, ε isoform of protein kinase C; OGD, oxygen-glucose deprivation; DIV, days *in vitro*.

acute OGD treatment (Fig. 2), which indicated that the function of the dendritic spine was damaged.

Acute OGD increases PKCε kinase activity and protein expression levels in primary neuronal culture. The present study investigated how acute OGD treatment regulates PKCε. High-density cortical neurons at DIV17 were treated with OGD for 2 h before measuring PKCε protein level and activity, respectively by western blotting and kinase activity assay Following 2 h treatment, the kinase activity of PKCε significantly increased compared with that in the control (Fig. 3A). In addition, protein expression of PKCε was also significantly increased after 2 h OGD treatment (Fig. 3B and C).

Inhibition of PKCε activity following acute OGD rescues dendritic spine dysfunction. To investigate whether functional change of PKCε induced dendritic spine dysfunction following OGD, we applied PKCε-specific inhibiting peptide, EAVSLKPT. This inhibiting peptide specifically blocks binding of PKCε with its downstream effecter, Rho-associated coiled-coil containing protein kinase 2, and thus inhibits PKCε function without interfering with its ATP-binding motif (20). Confocal microscopy results showed that the number of dendritic spines was significantly rescued by inhibitor pre-treatment (Fig. 4A and B). MTT assay showed that the cell viability did not change significantly following different treatments (Fig. 4C). Dendritic spine length and width were quantified in each group. OGD treatment significantly increased the mean spine length whereas the mean spine width was significantly decreased, indicating that the number of mature spines was significantly decreased in the OGD treatment group. On the other hand, dendritic spine defects caused by OGD treatment were decreased in cells pre-treated with PKCε inhibitor compared with those in the OGD treatment group (Fig. 4D and E). Electrophysiological analysis, which was performed to measure the function of dendritic spines from hippocampus neurons, showed that the decrease in mEPSC frequency due to the OGD treatment was abolished by the PKCε inhibitor pre-treatment, indicating that the synapse function was largely preserved following OGD with PKCε inhibitor pre-treatment (Fig. 5).

PKCε-induced RhoA activation mediates dendritic spine impairment following OGD. The morphology and function of dendritic spines are regulated by the cytoskeleton network and Rho-GTPases are key regulators of actin cytoskeleton rearrangement, which is the major structure maintaining dendritic spine morphology (21). To investigate if Rho-GTPases are involved in OGD, the activity of RhoA, Rac1 and CDC42 were measured following OGD. High-density cortical neurons at DIV17 were treated with OGD for 2 h. Cells were lysed and the same amount of protein was used to measure the active forms of RhoA, Rac1 and CDC42. Total RhoA, Rac1 and CDC42 protein levels were measured by western blotting as a control. Following OGD treatment, the activity of RhoA was significantly increased while the activity of Rac1 and CDC42 was not significantly different compared with that in the control (Fig. 6). Furthermore, the present study investigated if RhoA was downstream of PKCε by pre-treating cortical neurons with PKCε inhibitor peptide. Following 24 h PKCε inhibitor pre-treatment, activation of RhoA was blocked, indicating

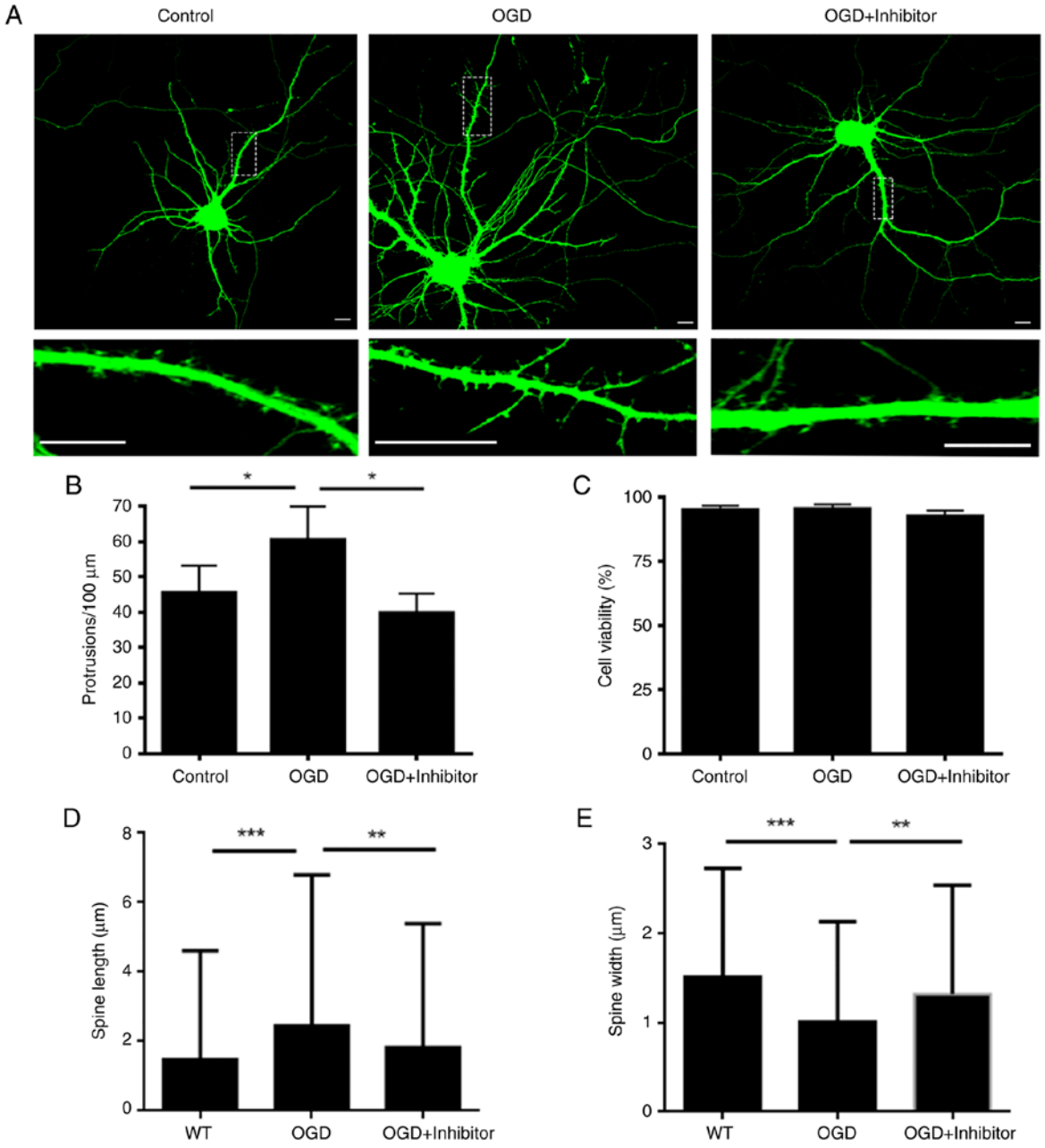

Figure 4. PKCε inhibitor prevents OGD-induced dendritic spine morphology impairment. (A) Primary hippocampus neurons were transfected with green fluorescent protein at DIV5 and treated with PKCε inhibitor for 24 h and then OGD for 2 h at DIV17. Cells were visualized by confocal microscopy (scale bar, 10 μm). Lower images represent magnifications of the dotted region of upper images. (B) Number of protrusions from each group was quantified. (C) High-density cortical neurons were treated with inhibitor and OGD at DIV17. MTT assay was then performed (n=3 batches of neurons). Quantification of spine (D) length and (E) width (n=1,200-1,500 protrusions from ≥20 neurons). *P<0.05, **P<0.01 and ***P<0.001. PKCε, ε isoform of protein kinase C; OGD, oxygen-glucose deprivation; DIV, days *in vitro*; WT, wild-type.

that RhoA is a downstream molecule of PKCε that mediates OGD-induced dendritic spine impairment (Fig. 6).

Discussion

Brain ischemia is a severe disorder that damages brain tissue and leads to neuronal death (19), triggering cognitive impairment or dementia that includes alterations in learning, memory and function needed to perform basic daily life activities (22). AD and brain ischemia are common pathologies of ageing and their frequent co-occurrence has been recognized (23,24). A previous study reported that patients with AD reporting cerebrovascular events exhibit more severe cognitive function decline compared with those without cerebrovascular events (25). Preclinical and clinical evidence has indicated that AD and brain ischemia may share common pathological pathways (26-29). However, to the best of our knowledge, the molecular mechanisms that connect these two diseases remain unclear.

The majority (>95%) of all excitatory synapses are located at dendritic spines and loss of excitatory synapses is a key characteristic of AD (30). Synapse dysfunction and dendritic spine loss are key early-stage symptoms of cognitive function impairments (31). Contrary to irreversible neuronal death,

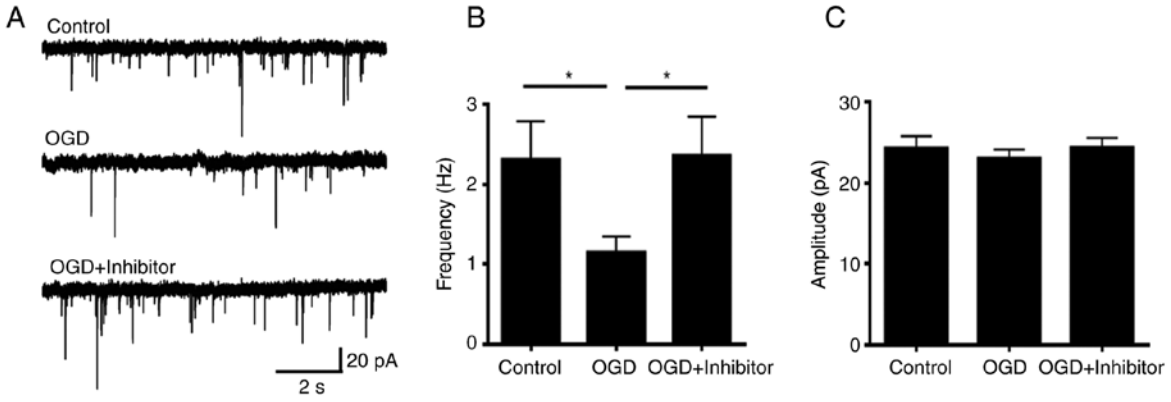

Figure 5. PKCε inhibitor prevents OGD-induced synapse dysfunction. (A) mEPSC was recorded on primary hippocampus neurons following OGD with or without PKCε inhibitor pre-treatment. (B) Current frequency and (C) amplitude were quantified (n=20-30 neurons). *P<0.05. PKCε, ε isoform of protein kinase C; OGD, oxygen-glucose deprivation; mEPSC, miniature excitatory postsynaptic current.

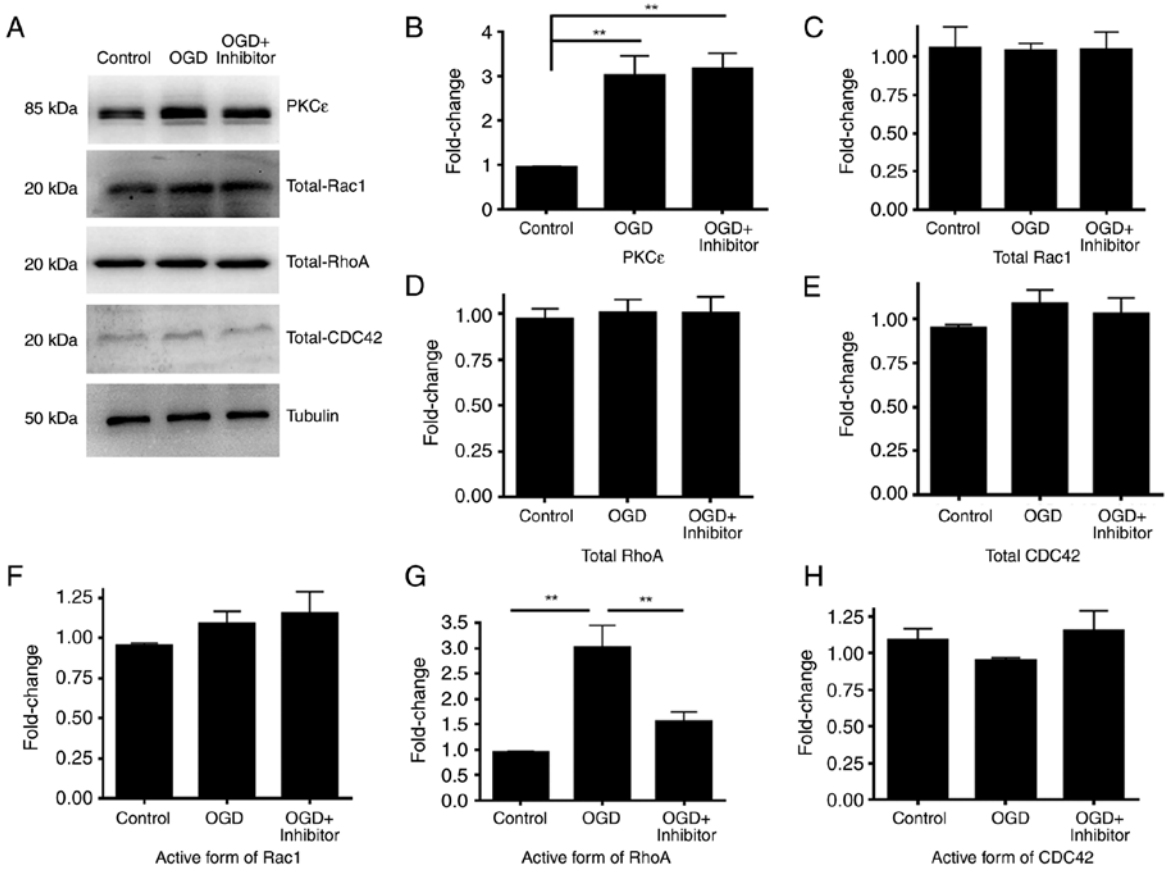

Figure 6. PKCε inhibitor regulates small-RhoGTPase activity. (A) High-density cortical neurons were treated with PKCε inhibitor for 24 h and OGD for 2 h. Cells were lysed for western blotting. Quantification of (B) PKCε; (C) total Rac1; (D) for total RhoA, and (E) for total CDC42. Activated form of (F) Rac1, (G) RhoA, and (H) CDC42 were measured using G-LISA kits. **P<0.01. n=3 for western blotting and n=5 for G-LISA. PKC, protein kinase C; Rac1, Rac Family Small GTPase 1; RhoA, Ras homolog gene family, member A; CDC42, cell division cycle 42.

synapse loss is a reversible process if treated at an early stage (32). The present study investigated dendritic spine morphology and synapse function following acute OGD, which distinguished this study from other studies that focused on ischemia-induced cell death (33-36).

Members of the PKC family are involved in basic cellular functions, such as cell metabolism and movements (37). Several studies found that several members of the PKC family are involved in the occurrence of AD (38-40). For example, PKCε was found to be downregulated in patients with AD and a chemical agonist of PKCε, bryostatin 1, is now under clinical trial for AD treatment (41). A previous study also found that PKCε negatively regulates dendritic spine function through RhoA and Ephexin5 activation in the embryonic development stage (42). The present study used cultured neurons at DIV17, which were considered mature *in vitro* (43). PKCε activity was

found to be significantly upregulated following acute OGD, which may underlie the association between PKCε and brain ischemia-induced cognitive function impairment.

Previous studies have indicated that following heart ischemia, the hypoxia-inducible factor-1α upregulates PKCε through epigenetic modifications and then impairs mitochondrial function in cardiocytes (44). Furthermore, studies also showed that a calcium signal in neurons is upregulated following hypoxia, which may also regulate the protein expression of PKCε in neurons (45-47). Considering that the changes in protein generation usually occur days after stimulation, it was hypothesized that the increase in the PKCε protein levels at acute phase after 2 h OGD treatment was due to inhibition of PKCε degradation. This should be further investigated in future studies.

The present study used the term 'protrusion' to represent all types of dendritic spine dynamics, which include a mature spine with a typical mushroom shape, an immature spine with a typical thin shape, a newly formed spine with stubby shape, as well as the non-functional filopodia and all other atypical shapes (48). Due to the limited image resolution, further separation into sub-groups was not possible. Because all the aforementioned types of protrusions represent a certain moment of the spine dynamics, the present study calculated the number of matured spines vs. all protrusions to quantified the percentage of mature spine.

In conclusion, an OGD cell model in primary neuronal culture was established in the present study to simulate adult brain ischemia *in vitro*. Dendritic spine of the hippocampus and cortical neurons was impaired following acute phase of OGD treatment. Concomitantly, PKCε protein levels and activity were also increased. Furthermore, inhibiting the function of PKCε ameliorated excitatory synapse dysfunction caused by OGD treatment. Finally, activity of RhoA, but not that of Rac1 or CDC42, was increased following PKCε activation. The findings of the present study may suggest novel therapeutic targets for synapse dysfunction and cognitive loss following brain ischemia.

Acknowledgements

Not applicable.

Funding

The present study was supported by the Huzhou Science And Technology Grant (grant no. 2020GZ42).

Availability of data and materials

The datasets used and/or analysed during the current study are available from the corresponding author on reasonable request.

Authors' contributions

SW designed the study and drafted the manuscript. SW and YW confirm the authenticity of all the raw data. XW designed the study and performed cell culture, electrophysiology recording and imaging. CG performed imaging studies. LL performed the primary cell culture and blinded dendritic spine numbering. MQ performed the statistical analysis. GS performed blinded dendritic spine numbering. YW designed the electrophysiology study. All authors have read and approved the final manuscript.

Ethics approval and consent to participate

Procedures involving animals were approved by the Institutional Animal Care and Use Committee of WuXi AppTec Co., Ltd. (Qidong site, Jiangsu, China; approval no. GP01-QD089-2022v1.0).

Patient consent for publication

Not applicable.

Competing interests

The authors declare that they have no competing interests.

References

1. Kalaria RN, Akinyemi R and Ihara M: Stroke injury, cognitive impairment and vascular dementia. Biochim Biophys Acta 1862: 915-925, 2016.
2. Kalaria RN: The role of cerebral ischemia in Alzheimer's disease. Neurobiol Aging 21: 321-330, 2000.
3. Pluta R, Januszewski S and Czuczwar SJ: Brain ischemia as a prelude to Alzheimer's disease. Front Aging Neurosci 13: 636653, 2021.
4. Pluta R, Jabłoński M, Ułamek-Kozioł M, Kocki J, Brzozowska J, Januszewski S, Furmaga-Jabłońska W, Bogucka-Kocka A, Maciejewski R and Czuczwar SJ: Sporadic Alzheimer's disease begins as episodes of brain ischemia and ischemically dysregulated Alzheimer's disease genes. Mol Neurobiol 48: 500-515, 2013.
5. Mungas D, Jagust WJ, Reed BR, Kramer JH, Weiner MW, Schuff N, Norman D, Mack WJ, Willis L and Chui HC: MRI predictors of cognition in subcortical ischemic vascular disease and Alzheimer's disease. Neurology 57: 2229-2235, 2001.
6. Qi JP, Wu H, Yang Y, Wang DD, Chen YX, Gu YH and Liu T: Cerebral ischemia and Alzheimer's disease: The expression of amyloid-beta and apolipoprotein E in human hippocampus. J Alzheimers Dis 12: 335-341, 2007.
7. Pluta R, Ułamek-Kozioł M and Czuczwar SJ: Neuroprotective and neurological/cognitive enhancement effects of curcumin after brain ischemia injury with Alzheimer's disease phenotype. Int J Mol Sci 19: 4002, 2018.
8. Jiang T, Handley E, Brizuela M, Dawkins E, Lewis KEA, Clark RM, Dickson TC and Blizzard CA: Amyotrophic lateral sclerosis mutant TDP-43 may cause synaptic dysfunction through altered dendritic spine function. Dis Model Mech 12: dmm038109, 2019.
9. Reza-Zaldivar EE, Hernández-Sápiens MA, Minjarez B, Gómez-Pinedo U, Sánchez-González VJ, Márquez-Aguirre AL and Canales-Aguirre AA: Dendritic spine and synaptic plasticity in Alzheimer's disease: A focus on MicroRNA. Front Cell Dev Biol 8: 255, 2020.
10. Pedrazzoli M, Losurdo M, Paolone G, Medelin M, Jaupaj L, Cisterna B, Slanzi A, Malatesta M, Coco S and Buffelli M: Glucocorticoid receptors modulate dendritic spine plasticity and microglia activity in an animal model of Alzheimer's disease. Neurobiol Dis 132: 104568, 2019.
11. Niftullayev S and Lamarche-Vane N: Regulators of Rho GTPases in the nervous system: Molecular implication in axon guidance and neurological disorders. Int J Mol Sci 20: 1497, 2019.
12. Gao K, Liu M, Ding Y, Yao M, Zhu Y, Zhao J, Cheng L, Bai J, Wang F, Cao J, *et al*: A phenolic amide (LyA) isolated from the fruits of Lycium barbarum protects against cerebral ischemia-reperfusion injury via PKCε/Nrf2/HO-1 pathway. Aging (Albany NY) 11: 12361-12374, 2019.
13. Lancaster TS, Jefferson SJ and Korzick DH: Local delivery of a PKCε-activating peptide limits ischemia reperfusion injury in the aged female rat heart. Am J Physiol Regul Integr Comp Physiol 301: R1242-R1249, 2011.

14. Akaike A: Preclinical evidence of neuroprotection by cholinesterase inhibitors. Alzheimer Dis Assoc Disord 20 (2 Suppl 1): S8-S11, 2006.
15. Villalba HAlbekairi T, Vaidya B and Abbruscato TJ: Role of Myo-inositol in ischemic stroke outcome in a preclinical tobacco smoke exposed mouse model. FASEB J 33 (S1): S500.2, 2019.
16. Babu M, Singh N and Datta A: In vitro oxygen glucose deprivation model of ischemic stroke: A proteomics-driven systems biological perspective. Mol Neurobiol 59: 2363-2377, 2022.
17. Sun M, Bernard LP, Dibona VL, Wu Q and Zhang H: Calcium phosphate transfection of primary hippocampal neurons. J Vis Exp: e50808, 2013.
18. Juntunen M, Hagman S, Moisan A, Narkilahti S and Miettinen S: In vitro oxygen-glucose deprivation-induced stroke models with human neuroblastoma cell- and induced pluripotent stem cell-derived neurons. Stem Cells Int 2020: 8841026, 2020.
19. Niizuma K, Yoshioka H, Chen H, Kim GS, Jung JE, Katsu M, Okami N and Chan PH: Mitochondrial and apoptotic neuronal death signaling pathways in cerebral ischemia. Biochim Biophys Acta 1802: 92-99, 2010.
20. Rechfeld F, Gruber P, Kirchmair J, Boehler M, Hauser N, Hechenberger G, Garczarczyk D, Lapa GB, Preobrazhenskaya MN, Goekjian P, *et al*: Thienoquinolines as novel disruptors of the PKCε/RACK2 protein-protein interaction. J Med Chem 57: 3235-3246, 2014.
21. Nayak RC, Chang KH, Vaitinadin NS and Cancelas JA: Rho GTPases control specific cytoskeleton-dependent functions of hematopoietic stem cells. Immunol Rev 256: 255-268, 2013.
22. Kawabori M and Yenari MA: Inflammatory responses in brain ischemia. Curr Med Chem 22: 1258-1277, 2015.
23. Vijayan M and Reddy PH: Stroke, vascular dementia, and Alzheimer's disease: Molecular links. J Alzheimers Dis 54: 427-443, 2016.
24. Takizawa C, Gemmell E, Kenworthy J and Speyer R: A systematic review of the prevalence of oropharyngeal dysphagia in stroke, Parkinson's disease, Alzheimer's disease, head injury, and pneumonia. Dysphagia 31: 434-441, 2016.
25. Zhang X, Zhou K, Wang R, Cui J, Lipton SA, Liao FF, Xu H and Zhang YW: Hypoxia-inducible factor 1alpha (HIF-1alpha)-mediated hypoxia increases BACE1 expression and beta-amyloid generation. J Biol Chem 282: 10873-10880, 2007.
26. Zlokovic BV and Griffin JH: Cytoprotective protein C pathways and implications for stroke and neurological disorders. Trends Neurosci 34: 198-209, 2011.
27. Hook V, Yoon M, Mosier C, Ito G, Podvin S, Head BP, Rissman R, O'Donoghue AJ and Hook G: Cathepsin B in neurodegeneration of Alzheimer's disease, traumatic brain injury, and related brain disorders. Biochim Biophys Acta Proteins Proteom 1868: 140428, 2020.
28. Fu Z, Caprihan A, Chen J, Du Y, Adair JC, Sui J, Rosenberg GA and Calhoun VD: Altered static and dynamic functional network connectivity in Alzheimer's disease and subcortical ischemic vascular disease: Shared and specific brain connectivity abnormalities. Hum Brain Mapp 40: 3203-3221, 2019.
29. Manda-Handzlik A and Demkow U: The brain entangled: The contribution of neutrophil extracellular traps to the diseases of the central nervous system. Cells 8: 1477, 2019.
30. Rochefort NL and Konnerth A: Dendritic spines: From structure to in vivo function. EMBO Rep 13: 699-708, 2012.
31. Counts SE, Nadeem M, Lad SP, Wuu J and Mufson EJ: Differential expression of synaptic proteins in the frontal and temporal cortex of elderly subjects with mild cognitive impairment. J Neuropathol Exp Neurol 65: 592-601, 2006.
32. Qi Y, Yu S, Du Z, Qu T, He L, Xiong W, Wei W, Liu K and Gong S: Long-term conductive auditory deprivation during early development causes irreversible hearing impairment and cochlear synaptic disruption. Neuroscience 406: 345-355, 2019.
33. Forouzanfar F, Asadpour E, Hosseinzadeh H, Boroushaki MT, Adab A, Dastpeiman SH and Sadeghnia HR: Safranal protects against ischemia-induced PC12 cell injury through inhibiting oxidative stress and apoptosis. Naunyn Schmiedebergs Arch Pharmacol 394: 707-716, 2021.
34. Li C, Sun G, Chen B, Xu L, Ye Y, He J, Bao Z, Zhao P, Miao Z, Zhao L, *et al*: Nuclear receptor coactivator 4-mediated ferritinophagy contributes to cerebral ischemia-induced ferroptosis in ischemic stroke. Pharmacol Res 174: 105933, 2021.
35. Lee ML, Sulistyowati E, Hsu JH, Huang BY, Dai ZK, Wu BN, Chao YY and Yeh JL: KMUP-1 ameliorates ischemia-induced cardiomyocyte apoptosis through the NO-cGMP-MAPK signaling pathways. Molecules 24: 1376, 2019.
36. Dietz RM, Cruz-Torres I, Orfila JE, Patsos OP, Shimizu K, Chalmers N, Deng G, Tiemeier E, Quillinan N and Herson PS: Reversal of global ischemia-induced cognitive dysfunction by delayed inhibition of TRPM2 ion channels. Transl Stroke Res 11: 254-266, 2020.
37. Rosse C, Linch M, Kermorgant S, Cameron AJ, Boeckeler K and Parker PJ: PKC and the control of localized signal dynamics. Nat Rev Mol Cell Biol 11: 103-112, 2010.
38. Ortiz-Sanz C, Balantzategi U, Quintela-López T, Ruiz A, Luchena C, Zuazo-Ibarra J, Capetillo-Zarate E, Matute C, Zugaza JL and Alberdi E: Amyloid β/PKC-dependent alterations in NMDA receptor composition are detected in early stages of Alzheimer's disease. Cell Death Dis 13: 253, 2022.
39. Sasahara T, Satomura K, Tada M, Kakita A and Hoshi M: Alzheimer's Aβ assembly binds sodium pump and blocks endothelial NOS activity via ROS-PKC pathway in brain vascular endothelial cells. iScience 24: 102936, 2021.
40. Sajan MP, Braun U, Leitges M, Park C, Diamond DM, Wu J, Hansen BC, Duncan MA, Apostolatos CA, Apostolatos AH, *et al*: Atypical PKC controls β-secretase expression and thereby regulates production of Alzheimer plaque precursor Aβ in brain and insulin receptor degradation in liver. Metab Clin Exper 104 (Suppl): S154112, 2020.
41. Schrott LM, Jackson K, Yi P, Dietz F, Johnson GS, Basting TF, Purdum G, Tyler T, Rios JD, Castor TP and Alexander JS: Acute oral bryostatin-1 administration improves learning deficits in the APP/PS1 transgenic mouse model of Alzheimer's disease. Curr Alzheimer Res 12: 22-31, 2015.
42. Schaffer TB, Smith JE, Cook EK, Phan T and Margolis SS: PKCε inhibits neuronal dendritic spine development through dual phosphorylation of Ephexin5. Cell Rep 25: 2470-2483.e8, 2018.
43. Liao MH, Xiang YC, Huang JY, Tao RR, Tian Y, Ye WF, Zhang GS, Lu YM, Ahmed MM, Liu ZR, *et al*: The disturbance of hippocampal CaMKII/PKA/PKC phosphorylation in early experimental diabetes mellitus. CNS Neurosci Ther 19: 329-336, 2013.
44. McCarthy J, Lochner A, Opie LH, Sack MN and Essop MF: PKCε promotes cardiac mitochondrial and metabolic adaptation to chronic hypobaric hypoxia by GSK3β inhibition. J Cell Physiol 226: 2457-2468, 2011.
45. Sommer N, Strielkov I, Pak O and Weissmann N: Oxygen sensing and signal transduction in hypoxic pulmonary vasoconstriction. Eur Respir J 47: 288-303, 2016.
46. Mungai PT, Waypa GB, Jairaman A, Prakriya M, Dokic D, Ball MK and Schumacker PT: Hypoxia triggers AMPK activation through reactive oxygen species-mediated activation of calcium release-activated calcium channels. Mol Cell Biol 31: 3531-3545, 2011.
47. Shimoda LA and Undem C: Interactions between calcium and reactive oxygen species in pulmonary arterial smooth muscle responses to hypoxia. Respir Physiol Neurobiol 174: 221-229, 2010.
48. Sanchez-Arias JC, Candlish RC, van der Slagt E and Swayne LA: Pannexin 1 regulates dendritic protrusion dynamics in immature cortical neurons. eNeuro 7: ENEURO.0079-20.2020, 2020.